ISBN: 978-3-95450-227-1 ISSN: 2673-5490 doi:10.18429/JACoW-IPAC2022-WEOZGD1

DESIGN OF AN LPA-BASED FIRST-STAGE INJECTOR FOR A SYNCHROTRON LIGHT SOURCE

Xueyan Shi[1,2,*], Haisheng Xu[1,†]
[1]Institute of High Energy Physics, Chinese Academy of Sciences, Beijing, China
[2]University of Chinese Academy of Sciences, Beijing, China

Abstract

Study of plasma-based acceleration has been a frontier of accelerator community for decades. The beam quality obtained from a laser-plasma accelerator (LPA) becomes higher and higher. Nowadays, the combination of LPAs and the conventional RF accelerators attracts quite some research interests. One of the interesting directions to go is to replace the LINAC of a synchrotron light source by an LPA. However, there are still challenges, e.g., the energy stability of the electron bunches, to be solved. In this paper, we present a preliminary physical design of a 500 MeV LPA-based first-stage injector for a synchrotron light source. Preliminary study for suppressing the energy deviation of the electron bunches generated by LPA is also presented.

INTRODUCTION

Laser-plasma accelerator (LPA) has become an important direction in future particle accelerators because of the high accelerating gradient. In the past years, there were many researches for improving the beam quality of LPAs, such as the beam energy [1], energy stability [2] and bunch charge. The future LPAs are expected to be used in many applications, such as FELs, light sources, and colliders. We are interested in the application of LPAs in synchrotron light sources.

Synchrotron light sources have been widely used in different fields. As far as we know, most of the existing synchrotron light sources consist of LINACs, booster synchrotrons, and storage rings. The LINACs and boosters are usually called the "injectors" of the storage rings, which are used to generate electron bunches and to accelerate electron bunches to the desired energy of the storage rings. It would be very interesting if the injectors of storage rings can be replaced by LPAs because it would reduce the size of the injector significantly. However, it requires several GeV level beam energy and very good stability to the LPA. Therefore, we believe that it's reasonable to consider using an LPA to replace the injector of booster (LINAC) as the starting point, saying, lower expectation at the beginning.

However, the few percent level central energy jitter and energy spread of electron bunches generated by LPAs (e.g., approximately 2.4% central energy jitter and 4% energy spread presented in [2]) are still not small enough for injection into the booster (a typical value of energy acceptance ±3%). Several schemes [3–6], therefore, were proposed to suppress the energy spread of electron bunches, such as the passive plasma dechirper which can reduce the energy spread but not the central energy deviation. One of the most promising approaches is to combine a chicane with an active dechirper [7, 8], this scheme, in principle, can reduce not only the energy spread but also the central energy jitter of electron bunches. The principle is to add a nearly linear negative energy chirp (energy-position correlation, the energy of particles decrease from bunch head to tail) to the bunch by a chicane with positive R_{56} (high energy particles will run to the head and the lows will run to the tail), then use the longitudinal wakefield generated by the dechirper to compensate the chirp, so as to reduce the energy deviation. On this basis, in order to meet the demands of synchrotron light sources, we wonder whether the scheme works if we keep increasing the charge of the injected electron bunch.

We found that there are three main challenges: (1) the severe beam loading effect will destroy the linearity of longitudinal wakefield E_z in the active plasma dechirper (APD) which works in the nonlinear regime; (2) the bunch length is subjected to the plasma wavelength of APD, which in turn is limited by the increasing laser peak power; (3) the chromatic effect in the quadrupoles makes it difficult to focus the RMS beam size within the radius of the plasma bubble.

Here we present the preliminary design of a beamline starting from a LPA, followed by a triplet, a magnetic chicane, and an APD, showed in Fig. 1. The rest of this manuscript is arranged as follows: Section II gave the typical parameters of an electron bunch, which was used as the initial bunch in the following design and simulations, generated by an LPA. Then, the considerations in the selection of the main parameters were described in Section III, followed by the basic design of the Twiss parameters of the beamline in Section IV. Section V showed the main simulations results in the APD. Conclusions and discussions were given in Section VI.

Figure 1: Elements from left to right: laser plasma accelerator, triplet, chicane and active plasma dechirper.

ELECTRON BUNCH FROM AN LPA

Since it's a very big topic to study how to generate high quality electron bunches in a LPA, we didn't really go into details of this topic. We just assume that the LPA can provide the initial electron beams we used which are not from the LPA simulations but generated by MATLAB according to a set of LPA beam parameters [4, 9]. The main parameters of

* shixueyan@ihep.ac.cn
† xuhs@ihep.ac.cn

ISBN: 978-3-95450-227-1 ISSN: 2673-5490 doi:10.18429/JACoW-IPAC2022-WEOZGD1

the generated electron bunch are listed in Table 1. Figure 2 shows the longitudinal phase space and the transverse real space of the generated electron bunch.

Table 1: Initial Beam Parameters

Parameters	Value
Beam design energy	500 MeV
RMS energy spread	0.94 %
Norm. RMS emittance	2 μmrad
RMS bunch length	2 μm
RMS beam size	2.2 μm

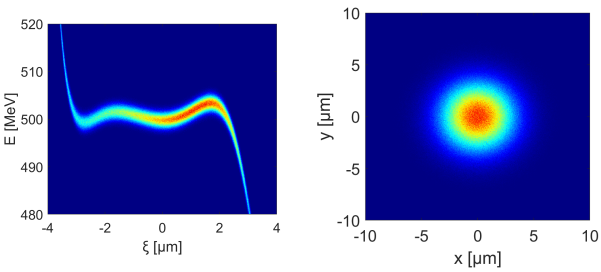

Figure 2: The longitudinal phase space and transverse x-y real space of the initial electron beam generated by MATLAB.

PARAMETERS SELECTION

Through rough estimations and simulations, we find that the APD parameters play a decisive role in the parameters selection of the whole design.

Since the APD is driven by a laser pulse and the plasma density doesn't have to match with the laser, we started the consideration from the laser parameters (peak power P and spot size w_0) and the plasma parameters (plasma density n_p) simultaneously. We summarized three trade-offs to decide these three main parameters. To get a larger dechirping strength ($\frac{dE_z}{d\xi}$, the slope of the longitudinal wakefield provided by APD) which avails to weaken the beam loading effect mentioned in the last section, one should choose a: (1) larger P, meanwhile a higher cost and difficulty; (2) smaller w_0, meanwhile need to focus the electron beam to a smaller size in transverse direction; (3) larger n_p, meanwhile generate a strong limit to the bunch length which is not conducive to weaken the beam loading effect. Considered the trade-offs, the final APD parameters we thought reasonable are a laser peak power P = 150 TW, a laser wavelength λ_0 = 800 nm, a pulse duration τ = 25 fs, a laser spot size at focus $w_0 = 33.4\mu m$, resulting in a peak normalized vector potential of a_0 = 2. By simulations, we chose a plasma density $n_p = 2.5 \times 10^{16} cm^{-3}$ for the APD. Actually, at the same set of laser parameters, according to the formula $e\frac{dE_z}{d\xi}L = \frac{dW}{d\xi}$, where e the elementary charge, L the length of the APD, $\frac{dW}{d\xi}$ the energy chirp of the bunch added by the chicane, ξ is the longitudinal coordinate of the particle, the higher the n_p is, the higher the $\frac{dE_z}{d\xi}$ is and the shorter the length of the bubble will be, which means a smaller $d\xi$ then a larger $\frac{dW}{d\xi}$ if keep the maximum energy deviation dW unchanged in the electron bunch. So one may need to do simulations to choose an appropriate L. In addition, the formula above will not be user-friendly when the beam loading effect becomes heavier resulting in a nonlinear longitudinal wakefield E_z in the APD, because in that case, the $\frac{dE_z}{d\xi}$ isn't a constant at each ξ anymore.

BEAMLINE

According to the parameters selection in last section, we determined a $R_{56} = (dE/d\xi)^{-1} = 2mm$. Since $R_{56} \approx 2\theta^2(\Delta L + 2L_B/3)$ [10], with the artificial length of the magnetic dipole L_B, and the calculated bending angle for reference particle θ, one can calculates the drift length ΔL between the 1st (3rd) and the 2nd (4th) dipole in the chicane. Then we did twiss matching for this beamline by code ELEGANT to get the optimized strength of the quadrupoles which listed in Table 2. Figure 3 shows the evolution of twiss parameters along the beamline.

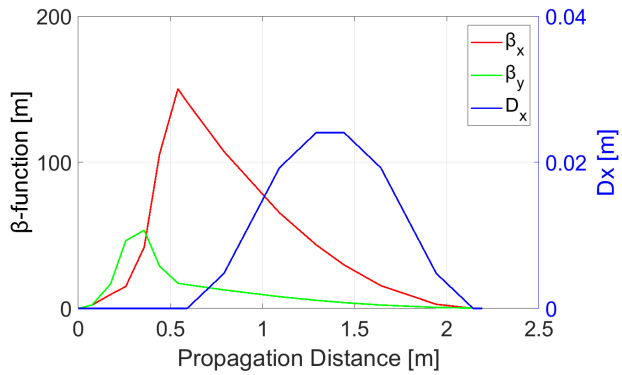

Figure 3: The evolution of twiss parameters along the beamline.

Table 2: Magnets in Beamline

Magnet	Length	Strength
Quad 1	0.1 m	45 T/m
Quad 2	0.1 m	69 T/m
Quad 3	0.1 m	45 T/m
Dipole 1-4	0.2 m	0.4 T

Since the chromaticity of the present beamline wasn't corrected, two new issues have arisen: (1) the beam size of the 500 MeV bunch was too large, which won't affect the beam transport in the APD but the statistical results of the central energy and the energy spread of the bunches because the particles beyond the bubble won't experience the wakefield to gain energy compensation so that the final transfer efficiency will be reduced further; (2) bunches with same inital beam size but different central energy will be focused to different

ISBN: 978-3-95450-227-1 ISSN: 2673-5490 doi:10.18429/JACoW-IPAC2022-WEOZGD1

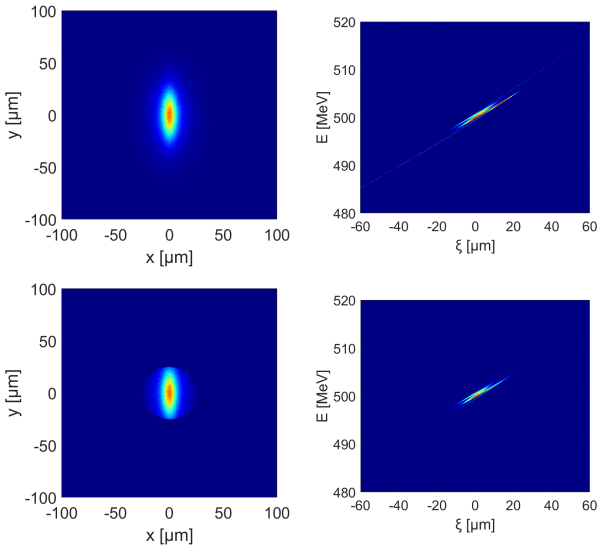

Figure 4: The transverse x-y real space (left) and the longitudinal phase space (right) of the electron beam with central energy of 500 MeV before (top) and after (bottom) the pinhole.

final beam sizes at the exit of the beamline resulting in different degrees of beam loading effect in the APD. Therefore, aiming to the two issues, (1) we calculated the relationship between the energy deviation and the arrival time of particles and made a translation to both the ξ and δ dimensions of the 500 MeV particle to get the ξ and δ of other energy particles to ensure that bunches with different central energy have the same transfer efficiency; (2) we tentatively added an pinhole with radius of 25 μm between the chicane and the APD to cut off the particles beyond the bubble, resulting in a beam transfer efficiency approximately 60 %. The corresponding transverse real space and longitudinal phase space are showed in Fig. 4. Following the above approaches, we prepared seven electron bunches of different central energy jitter from -2% to +3% with the transfer efficiency errors caused by the energy collimator less than 0.33%.

In future work, we will try to use sextupoles placed at the center of the chicane and add another triplet at the entrance of the APD to study whether these methods can solve these problems in our design.

ACTIVE PLASMA DECHIRPER SIMULATIONS FOR DIFFIERENT BUNCH CHARGE

We did simulation of the APD for different bunch charge by code WarpX.

50 pC

We first did a simulation for an electron bunch at a relative low charge of 50 pC, with central energy of 500 MeV to see how it works.

To find a suitable phase for this bunch is the first step. Due to the beam loading effect, the zero point of the field isn't as the same position as the no loading situation. Choosing different p hase w ill g ive d ifferent le ngth of AP D. In gen-eral, when suffering from a heavier beam loading effect, we choose the phase that can keep the central energy of the bunch with design energy unchanged.

The simulation result shows that the central energy deviation was reduced from 0.51 MeV to 0.22 MeV and the energy spread was suppressed from 0.29% to 0.24%. The almost constant energy spread is the result of the almost "flattened" effective E_z , showed in Fig. 5. Wherever the particles, at bunch head for high energy or bunch tail for low energy, they see the same value of E_z , which means that particles with different energy deviation experience almost the same energy compensation, hence the energy spread can not be effectively suppressed.

Then we tested the effectiveness of the APD for an electron bunch with central energy of 510 MeV. The simulation shows that the central energy deviation can be finally reduced down to 0.01 MeV. However, the energy spread increased from 0.29% to 0.36%.

Then we tested more central energy deviations in the range of ±2%. The significant reduction of the energy deviations of all the five cases can be seen in Fig. 6. Actually, each plasma bubble enters only one bunch at a time. For compar-ison purposes, we draw these bunches together. The specific final central energy deviations and energy spread are listed in Table 3. In addition, to let the bunch continue to propagate has no contribution to the elimination of the beam energy chirp, because the $\frac{dE_z}{d\xi}$ will decrease as the propagation distance of the laser increases, so the beam loading effect will become more obvious to even change the sign of the $\frac{dE_z}{d\xi}$, despite that the bunch charge doesn't change from beginning to end.

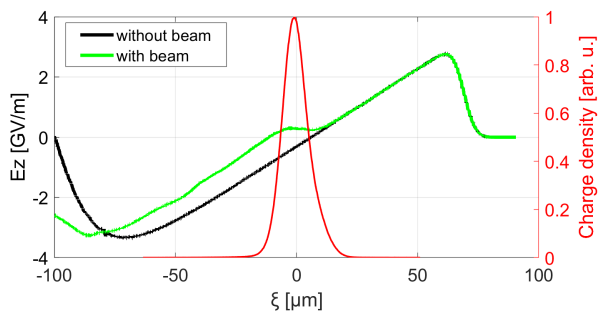

Figure 5: The E_z in the APD for 50 pC electron bunch with (green) and without (black) beam. The red line is the bunch charge density profile.

200 pC

Next, we increase the bunch charge up to 200 pC to see what will happen under a heavier beam loading. Actually, for the same APD, the selected phase is different from different bunch charges. Just because the zero phase changes with the charge, the range of central energy that can be held in the bubble varies. In general, the phase of the high charge bunch

ISBN: 978-3-95450-227-1 ISSN: 2673-5490 doi:10.18429/JACoW-IPAC2022-WEOZGD1

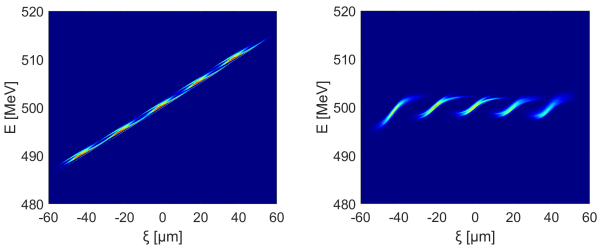

Figure 6: The longitudinal phase space before and after the APD ($L = 5.6mm$) of five 50 pC electron bunches with central energy deviations of -10 MeV, -5 MeV, 0 MeV, 5 MeV, 10 MeV, from left to right respectively.

Table 3: The final central energy deviation and energy spread after the APD of 50 pC bunches with initial central energy deviation from -10 MeV to 10 MeV

Designed Central Energy (MeV)	Central Energy Deviation (MeV)	Energy Spread
490	-0.68	0.41%
495	-0.19	0.28%
500	0.22	0.24%
505	0.05	0.24%
510	0.01	0.36%

is further back than that of the low charge bunch, which is further away from the laser. Therefore, for a higher bunch charge like 200 pC, the backward-moving phase makes it occur an offset to a slightly higher energy range, comparing to the above 50 pC situation. Figure 7 shows the E_z seen by each bunch when they propagated 2.3 mm long. We can see that the severe beam loading effect has severely disrupted linearity of E_z resulting in an increased energy spread but benefits the central energy deviation correction of bunch with high energy . The reason is that, for example, for the 510 MeV bunch, most of the particles in the bunch experience a higher E_z to get more energy compensation than it should have. Figure 8 shows the longitudinal phase space of five bunch with energy deviation from -10 MeV to 10 MeV before and after passing through the same APD. The specific initial and final central energy deviation and energy spread are listed in Table 4. The RMS central energy jitter and energy spread of these first five bunches are 0.83% and 1.20%. The RMS central energy jitter and energy spread of these last five bunches are 0.34% and 1.07%. Figure 9 and 10 are the corresponding longitudinal phase space and E_z of the last five bunches.

CONCLUSIONS AND DISCUSSIONS

Preliminary studies showed that the scheme chicane plus active plasma dechirper managed to reduce the central energy deviation and energy spread simultaneously for relatively low bunch charge situations such as 50 pC. The achieved energy spread now is still not as good as the previous work using X-band cavity as the dechirper because of

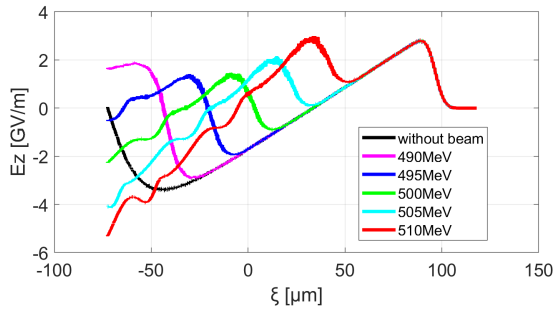

Figure 7: The longitudinal wakefield E_z in the APD for 200 pC electron bunches with different central energy.

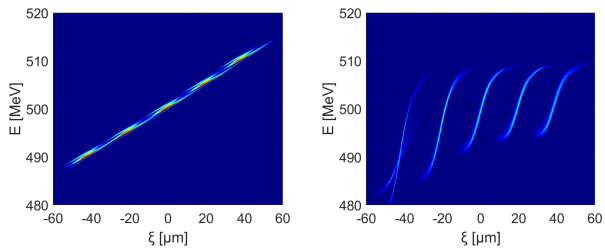

Figure 8: The longitudinal phase space before and after the APD ($L = 5.7mm$) of five 200 pC electron bunches with central energy deviations of -10 MeV, -5 MeV, 0 MeV, 5 MeV, 10 MeV, from left to right respectively.

Table 4: The final central energy deviation and energy spread after the APD of 200 pC bunches with initial central energy deviation from -10 MeV to 15 MeV

Designed Central Energy (MeV)	Central Energy Deviation (MeV)	Energy Spread
490	-8.50	1.50%
495	-3.49	1.39%
500	-0.44	1.07%
505	0.70	0.94%
510	1.10	0.90%
515	1.08	0.93%

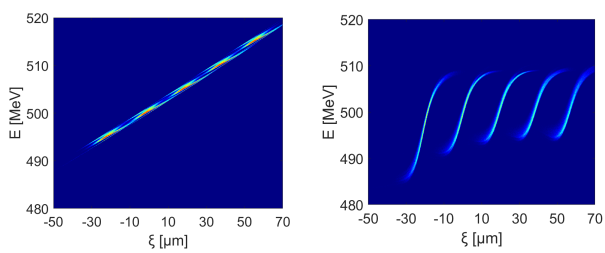

Figure 9: The longitudinal phase space before and after the APD ($L = 5.7mm$) of five 200 pC electron bunches with central energy deviations of -5 MeV, 0 MeV, 5 MeV, 10 MeV, 15 MeV from left to right respectively.

the short bunch length limited by the plasma density. However, it seems acceptable for the application as an injector of booster synchrotrons. Further optimizations of the APD de-

ISBN: 978-3-95450-227-1 ISSN: 2673-5490 doi:10.18429/JACoW-IPAC2022-WEOZGD1

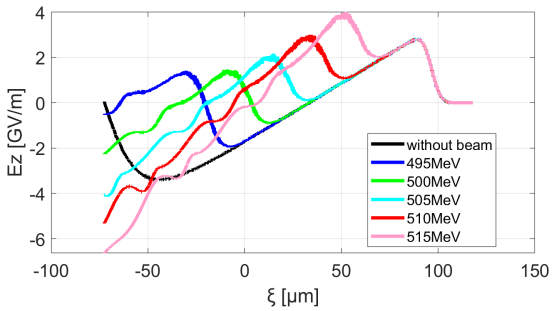

Figure 10: The longitudinal wakefield E_z in the APD for 200 pC electron bunches with different central energy.

sign may help control the energy spread better. We extended the study to higher charge situations, which was challenging due to heavier beam loading. Preliminary results showed that central energy deviation can be reduced even for 200 pC bunch. We found that the slightly off-energy operation could be help for controlling the final central energy because of the backward-moving zero point phase of E_z.

ACKNOWLEDGEMENTS

The work was supported by National Natural Science Foundation of China (No. 11805217).

The authors would like to thank Dr. Yi Jiao, Dr. Dazhang Li, Dr. Ming Zeng and Mr. Jia Wang from IHEP, Dr. Yipeng Wu and Dr. Fei Li from UCLA, Dr Shiyu Zhou from Tsinghua University for their valuable comments and suggestions.

REFERENCES

[1] A. J. Gonsalves *et al.*, "Petawatt Laser Guiding and Electron Beam Acceleration to 8 GeV in a Laser-Heated Capillary Discharge Waveguide", *Phys. Rev. Lett.,* vol. 122, p. 084801, Feb. 2019. doi:10.1103/PhysRevLett.122.084801

[2] A. R. Maier *et al.*, "Decoding Sources of Energy Variability in a Laser-Plasma Accelerator", *Phys. Rev. X,* vol 10, p. 031039, Aug. 2020. doi:10.1103/PhysRevX.10.031039

[3] R. D'Arcy *et al.*, "Tunable Plasma-Based Energy Dechirper", *Phys. Rev. Lett.*, vol 122, p. 034801, Jan. 2019. doi:10.1103/Phys-RevLett.122.034801

[4] V. Shpakov *et al.*, "Longitudinal Phase-Space Manipulation with Beam-Driven Plasma Wakefields", *Phys. Rev. Lett.,* vol 122, p. 114801, Mar. 2019. doi:10.1103/PhysRevLett.122.114801

[5] Y. P. Wu *et al.*, "Phase Space Dynamics of a Plasma Wakefield Dechirper for Energy Spread Reduction", *Phys. Rev. Lett.,* vol 122, p. 204804, May 2019. doi:10.1103/PhysRevLett.122.204804

[6] Y. P. Wu *et al.*, "Near-Ideal Dechirper for Plasma-Based Electron and Positron Acceleration Using a Hollow Channel Plasma", *Phys. Rev. Appl.,* vol 12, p. 064011, Dec. 2019. doi:10.1103/PhysRevApplied.12.064011

[7] S. A. Antipov *et al.*, "Design of a prototype laser-plasma injector for an electron synchrotron", *Phys. Rev. Accel. Beams.,* vol 24, p. 111301, Nov. 2019. doi:10.1103/PhysRevAc-celBeams.24.111301

[8] A. F. Pousa *et al.*, "Energy Compression and Stabilization of Laser-Plasma Accelerators", Jun. 2021. doi:10.48550/arXiv.2106.04177

[9] M. Kirchen *et al.*, "Optimal BeamLoading in a Laser-Plasma Accelerator", *Phys. Rev. Lett.,* vol 126, p. 174801, Apr. 2021. doi:10.1103/PhysRevLett.126.174801

[10] W. Chao *et al.*, "Handbook of accelerator physics and engineering", World Scientific, 2013, pp. 335